Food Hydrocolloids 117 (2021) 106718

Contents lists available at ScienceDirect

Food Hydrocolloids

journal homepage: http://www.elsevier.com/locate/foodhyd

Effects of polysaccharide charge density on the structure and stability of carboxymethylcellulose-casein nanocomplexes at pH 4.5 prepared with and without a pH-cycle

Nan Li, Qixin Zhong *

Department of Food Science, The University of Tennessee, Knoxville, TN, USA

ARTICLE INFO

Keywords:
Casein-polysaccharide complexes
Carboxymethylcellulose
Charge density
Chelation
pH cycle

ABSTRACT

Carboxymethylcellulose (CMC) can stabilize acidic casein dispersions but the CMC charge density effect has not been studied. The objective of the present work was to study the structure and stability of CMC-casein nanocomplexes at pH 4.5 using CMC with the degree of substitution (DS) of 0.7, 0.9, and 1.2. Dispersions were prepared at 1%w/v casein and casein:CMC mass ratios from 5:1 to 1:1 with and without a pH-cycle. The calcium chelating capacity of CMC was strengthened as the DS increased, which enhanced the partial disassociation of casein micelles and therefore improved the dispersion clarity. The lowest dispersion turbidity was observed at a casein:CMC mass ratio of 3:1 for all three kinds of CMC, and the pH-cycle, by alkalizing dispersion pH to 11.3 followed by acidifying to pH 4.5, further lowered the dispersion turbidity. Electrostatic attraction was the mechanism of complex formation at pH 4.5, and the CMC on the complex surface was critical to the stability against aggregation. Furthermore, increasing the DS of CMC resulted in smaller complexes and clearer dispersions. Particularly, the dispersions with a CMC:casein mass ratio of 3:1 after the pH-cycle had the absorbance at 600 nm of 1.25, 0.85, and 0.57, and the mean hydrodynamic diameter of 379, 392, and 188 nm at the DS of 0.7, 0.9, and 1.2 respectively; the increased DS also increased the stability of complexes against aggregation and precipitation at elevated ionic strengths, from 50 mM to 200 mM NaCl. The present findings may broaden the application of caseins in acidic systems.

1. Introduction

Protein-polysaccharide complexes are very important for food formulations (Huang et al., 2019; Wang, Nian, et al., 2019) and have been studied for numerous biopolymers, mainly as a function of pH and protein-polysaccharide mass ratio (Kaushik, Dowling, Barrow, & Adhikari, 2015; Timilsena, Wang, Adhikari, & Adhikari, 2016). Electrostatic interaction is reported to be the major mechanism for the formation of protein-polysaccharide complexes, which is greatly affected by pH conditions and suppressed by the addition of salt (Kaushik et al., 2015; Souza & Garcia-Rojas, 2017; Wagoner & Foegeding, 2017). Besides the molecular structure of biopolymers, the protein-polysaccharide mass ratio determines the size of complexes, as well as the dispersion stability and viscosity of the overall system (Voron'ko, Derkach, Kuchina, & Sokolan, 2016). Forming complexes with polysaccharides can improve the dispersion stability of proteins around the isoelectric point (pI) and the thermal stability of proteins such as pea proteins and whey proteins (Lan, Chen, & Rao, 2018; Wagoner & Foegeding, 2017). In this work, properties and mechanisms of casein-carboxymethylcellulose (CMC) complexation are studied.

In bovine milk, α_{s1}-, α_{s2}-, β-, γ-, and κ-caseins are assembled as casein micelles, with the interior composed of mainly α_s- and β-caseins (Claeys et al., 2014; Dalgleish & Corredig, 2012). The serine residues of α_s- and β-caseins are extensively phosphorylated, making them sensitive to calcium ions, which is one of the major forces forming the micellar structure (Dalgleish, 2011). Excess calcium may lead to casein aggregation, while removal of calcium can cause the dissociation of casein micelles (Culler, Saricay, & Harte, 2017). The C-terminal fraction of κ-casein (residues 106–169), glycomacropeptide, is glycosylated and is highly hydrophilic to extend into the surrounding serum, while the other fraction is highly hydrophobic to interact with interior α_s- and β-caseins (Farrell et al., 2004). In native bovine milk with neutral pH, glycomacropeptide is negatively charged and highly stretched and forms a "hairy layer" on casein micelle surface to provide both electrostatic and

* Corresponding author. Department of Food Science The University of Tennessee 2510 River Drive Knoxville, TN, 37996, United States.
E-mail address: qzhong@utk.edu (Q. Zhong).

https://doi.org/10.1016/j.foodhyd.2021.106718
Received 5 November 2020; Received in revised form 24 February 2021; Accepted 25 February 2021
Available online 1 March 2021

steric repulsions to stabilize casein micelles against aggregation. Therefore, factors leading to the removal or collapse of this "hairy layer" can result in the instability and aggregation of casein micelles. For example, some proteolytic enzymes including pepsin and chymosin can cleave glycomacropeptide, and acidification causes the loss of effective net charges especially near to the pI of casein at around pH 4.6 (Farías, Martinez, & Pilosof, 2010). Casein aggregation is the physical basis of producing dairy products such as cheeses and yogurts, but is to be prevented in acidic beverages (Dalgleish, 2011).

Polysaccharides can be used to improve the stability of caseins at acidic conditions. Chitosan is the only natural cationic polysaccharide and can interact with overall negatively charged caseins between the pKa of chitosan at pH 6.5 and the pI of caseins through electrostatic attraction (Dhanasingh & Nallaperumal, 2010). More frequently, anionic polysaccharides with net negative charges in a wide pH range, such as soybean soluble polysaccharide and high methoxyl pectin (Cai, Wei, Guo, Ma, & Zhang, 2020; Liang & Luo, 2020), are used to improve the dispersion stability of caseins. Polysaccharides with carboxylate or sulfate groups are highly negatively charged above the pKa of 3.5 or 2.5 (Harnsilawat, Pongsawatmanit, & McClements, 2006; Nunes et al., 2017), respectively. Near or below the pI of casein, more positive charges of caseins become available for attraction by anionic polysaccharides. Even at neutral pH, electrostatic attraction can occur between carboxylate or sulfate groups of the polysaccharide and positively charged basic amino acid residues of caseins such as residues 97–112 of κ-casein (Jourdain, Schmitt, Leser, Murray, & Dickinson, 2009). In addition, the anionic groups of polysaccharides may bind calcium ions and therefore have the potential to chelate calcium from casein micelles (Li & Zhong, 2020a). The dissociation of casein micelles caused by chelating agents around neutral pH has been well studied and is significant to reduce the turbidity of casein micelle dispersions (Culler et al., 2017; Saricay, Hettiarachchi, Culler, & Harte, 2019).

CMC is an anionic polysaccharide derived from cellulose by substituting hydroxyl groups with carboxymethyl groups. Due to its non-toxicity, water solubility, and biodegradability, CMC is commonly used in food and non-food industries (Cai et al., 2011; Gibis, Schuh, & Weiss, 2015). CMC is a linear polyelectrolyte with the backbone composed of β(1 → 4)-linked glucopyranose residues and the negative charges provided by the substituting carboxymethyl groups. The degree of substitution (DS) of CMC is defined as the number of hydroxyl groups replaced by carboxymethyl groups per repeating unit and is usually in the range of 0.4–1.5 (An et al., 2014). The DS affects the solubility, emulsifying property, thickening property, stability, acid resistance, and salt tolerance of CMC (An et al., 2014; Cai, Wu, Du, & Zhang, 2018; Xin, Nie, Chen, Li, & Li, 2018). Especially, CMC with a higher DS has a higher charge density and shows the increased tendency to bind with positively charged molecules through electrostatic attraction (Xiong et al., 2017). CMC has been studied to improve the stability of acidified milk drinks, but these studies concentrate on the macroscopic phase behaviors during transition from neutral to acidic conditions (Du et al., 2007; Farrell et al., 2004), without elaborating mesoscopic particle structures and mechanisms of structural formation.

Furthermore, according to our previous study, casein micelles can be dissociated above pH 11.0 and caseins can re-associate to form smaller particles during the following acidification (Pan & Zhong, 2013). This pH-cycle method has been used to improve the stability and clarity of casein dispersions at pH 4.5 by forming nanocomplexes with propylene glycol alginate (PGA) or dextran sulfate (Li & Zhong, 2020a, 2020b). PGA and dextran sulfate are anionic polysaccharides with carboxylate and sulfate groups, respectively, and stabilized caseins at pH 4.5 by different mechanisms. PGA stabilized caseins by forming both covalent bonds and physical complexes, while dextran sulfate had chelating properties and formed core-shell structured nanocomplexes. As dextran sulfate is not a generally-recognized-as-safe (GRAS) food ingredient and the formation of covalent bonds with PGA can lower the nutritional quality of caseins, it is significant to study if the pH-cycle method can also apply to CMC, a commonly used GRAS food ingredient. Additionally, the availability of CMC products with different DSs allows, for the first time, the current study to concentrate on the impacts of charge density of polyelectrolytes on the structure and formation mechanisms of casein-polysaccharide complexes.

The overall objective of the present work was to study the impact of CMC charge density on the structure, stability, and formation mechanism of casein-CMC complexes prepared by adjusting pH directly from neutral to 4.5 (without the pH-cycle treatment) or initially to 11.30 and then 4.5 (the pH-cycle treatment). CMC preparations with the same molecular weight (MW) but three different DSs were studied, and dispersions were prepared with various casein to CMC mass ratios. The structure of casein-CMC complexes at pH 4.5 was characterized using dynamic light scattering (DLS), atomic force microscopy (AFM), and transmission electron microscopy (TEM). Chelating properties of CMC were studied by characterizing turbidity changes of dispersion at neutral pH before and after the pH-cycle treatment, free calcium ion concentration in micellar casein, CMC, and casein/CMC dispersions, and AFM particle morphology. Finally, the interactions between CMC and caseins were characterized for spectrophotometric analysis of methylene blue (MB) and the effects of ionic strength. Scientifically, this study illustrates mesoscopic structures and mechanisms of stable acidic casein dispersions enabled by CMC, as well as the impact of CMC charge density. Technologically, formulations and processes developed in the present study may be used to prepare practical translucent casein dispersions enabled with CMC.

2. Materials and methods

2.1. Materials

Micellar casein was a product from American Casein Company (Burlington, NJ). The casein sample contained 72.45 wt% protein according to the Kjeldahl analysis (AgSource Laboratories, Marshfield, WI), and 85.78% protein was determined to be caseins based on ImageJ (National Institutes of Health, Bethesda, MD) analysis of reducing sodium dodecyl sulfate polyacrylamide gel electrophoresis results. In addition, the casein sample had 6.80 wt% ash as measured using a Barnstead/Thermolyne muffle furnace FB1415M (Dubuque, IA) and 2.40 wt% calcium and 1.64 wt% phosphorus as determined with inductively coupled argon plasma (ICP) optical emission spectrometry (OES) 90 at the Water Quality Core Facility in the University of Tennessee (Knoxville, TN). The CMC sample with the MW of 250 kDa and DS of 1.2 was purchased from Sigma-Aldrich Corp. (St. Louis, Mo). Other two CMC samples with the same MW but DS of 0.7 and 0.9 were products of Acros Organics (Morris Plains, NJ). Other chemicals were from Sigma-Aldrich Corp. (St. Louis, Mo) or Fisher Scientific (Pittsburgh, PA).

2.2. Methods

2.2.1. Dispersion preparation

CMC stock solutions were prepared by stirring 1% w/v CMC powder in deionized water at room temperature (RT, ~21 °C) for about 10 h. To prepare dispersions with 1% w/v casein and casein:CMC mass ratios of 5:1, 4:1, 3:1, 2:1, and 1:1 (Li & Zhong, 2020a, 2020b), 100 mg micellar casein powder was mixed with appropriate volumes of the CMC stock solution and deionized water to a total volume of 10 mL, followed by stirring at 990 rpm on a magnetic stir plate (model Cimarec i Poly 15 and Multipoint Stirrers, Thermo Fisher Scientific, Waltham, MA) overnight (about 15 h) at RT. To avoid microbial contamination, 0.02% w/v NaN_3 was added in all dispersion samples. The pH value of the mixture dispersions was around 7.6 after the hydration.

The neutral mixture dispersions prepared as above were adjusted to pH 4.5 using two different methods. The pH-cycle method was adopted from our previous studies (Li & Zhong, 2020a, 2020b). Specifically, the neutral dispersions were alkalized to pH 11.3 using 20 μL of 4.0 M NaOH

and 10–30 μL of 2.0 M NaOH, followed by stirring at 990 rpm and RT for 1 h. Then the pH was decreased to 6.0, 5.0, and 4.5 successively using 1.0, 0.5, and 0.25 M citric acid. Citric acid was used because it resulted in smaller particles than hydrochloric acid during the pH-cycle treatment according to our previous study (Pan & Zhong, 2013). For samples without the pH-cycle treatment, the neutral dispersions were directly acidified to pH 4.5 using citric acid as described previously. During sample preparation, all dispersions were agitated at RT as described above. To simplify the description, casein/CMC_{DS} [x:y] is used to present the mixture dispersions, with the subscript number representing the DS of CMC and the casein:CMC mass ratio represented by x:y.

During the pH-cycle treatment, about 8.5 mM of citric acid was introduced when acidifying the casein/CMC [3:1] dispersion from pH 11.3 to pH 4.5. Therefore, a control dispersion was prepared by adding 8.5 mM sodium citrate in the neutral casein/CMC [3:1] sample and acidifying to pH 4.5 using 1.0 M HCl. The difference between this control dispersion and that going through the pH-cycle shows the net effect of the pH-cycle treatment in reducing the turbidity. Additionally, two casein and casein-CMC control dispersions at pH 7.6 were prepared for those without additional treatments after hydration (neutral-1) or alkalization to pH 11.3 followed by adjusting to pH 7.6 with 1.0 M citric acid (neutral-2).

2.2.2. Turbidity, particle size, and zeta potential measurements

The turbidity of dispersions at pH 4.5 was measured for the absorbance at 600 nm (A_{600}) with a UV–vis spectrophotometer (Evolution 201, Thermo Scientific, Waltham, MA) according to a previous method (Pan & Zhong, 2013). After diluting to 0.1% w/v overall biopolymer concentration with acidified deionized water that was pre-adjusted to pH 4.5 with 0.1 M citric acid, the particle size and zeta (ζ)-potential of casein/CMC dispersions and CMC solutions were measured using a model Zetasizer Nano-ZS90 instrument (Malvern Instruments Ltd., Worcestershire, UK).

2.2.3. Morphological studies

Morphological properties of casein, CMC, and their mixture systems at various pH conditions were studied using AFM following a previous study (Liu & Zhong, 2012) with some modifications. Neutral $CMC_{1.2}$, micellar casein, and casein/CMC [3:1] dispersions were diluted with deionized water to a total biopolymer content of 0.001%w/v. For casein/CMC [3:1] dispersions at pH 4.5, deionized water pre-acidified to pH 4.5 using 0.1 M citric acid was used for the dilution to a total biopolymer content of 0.001% w/v. Then 5 μL of the diluted dispersion was spread onto a freshly cleaved mica sheet which was mounted on a sample disk (Bruker Corp., Santa Barbara, CA). After the sample was dried in air overnight, a rectangular probe with a quoted force constant of 0.4 N/m was used to scan the sample. AFM images were generated at the "ScanAsyst in Air" mode (model Multimode 8, Bruker Corp., Santa Barbara, CA), and the images were analyzed with the NanoScope Analysis software (Version 1.50, Bruker Corp., Santa Barbara, CA).

Complementary to AFM analysis, transmission electron microscopy (TEM) was used to study the morphology of complexes. Briefly, deionized water preadjusted to pH 4.5 was used to dilute samples for 10 times, and one drop of the diluted sample was placed on a 200-mesh copper grid (FF200, Electron Microscopy Sciences, Hatfield, PA). After washing with deionized water, casein was stained using 1% uranyl acetate (Li & Zhong, 2020a). A JEM 1400-Flash electron microscope (JEOL Ltd., Tokyo, Japan) was used to capture TEM images.

2.2.4. Calcium-binding properties of CMC

Free calcium ion concentration was measured to study the calcium-chelating properties of CMC (Mekmene & Gaucheron, 2011). Each CMC stock solution was mixed with a 0.1 mM $CaCl_2$ solution to prepare solutions containing 0.33% w/v CMC and 1, 2, 5, 10 and 15 mM $CaCl_2$, followed by addition of deionized water to a total volume of 10 mL. After equilibration for 4 h at RT, 0.4 mL of perfectION calcium ionic strength

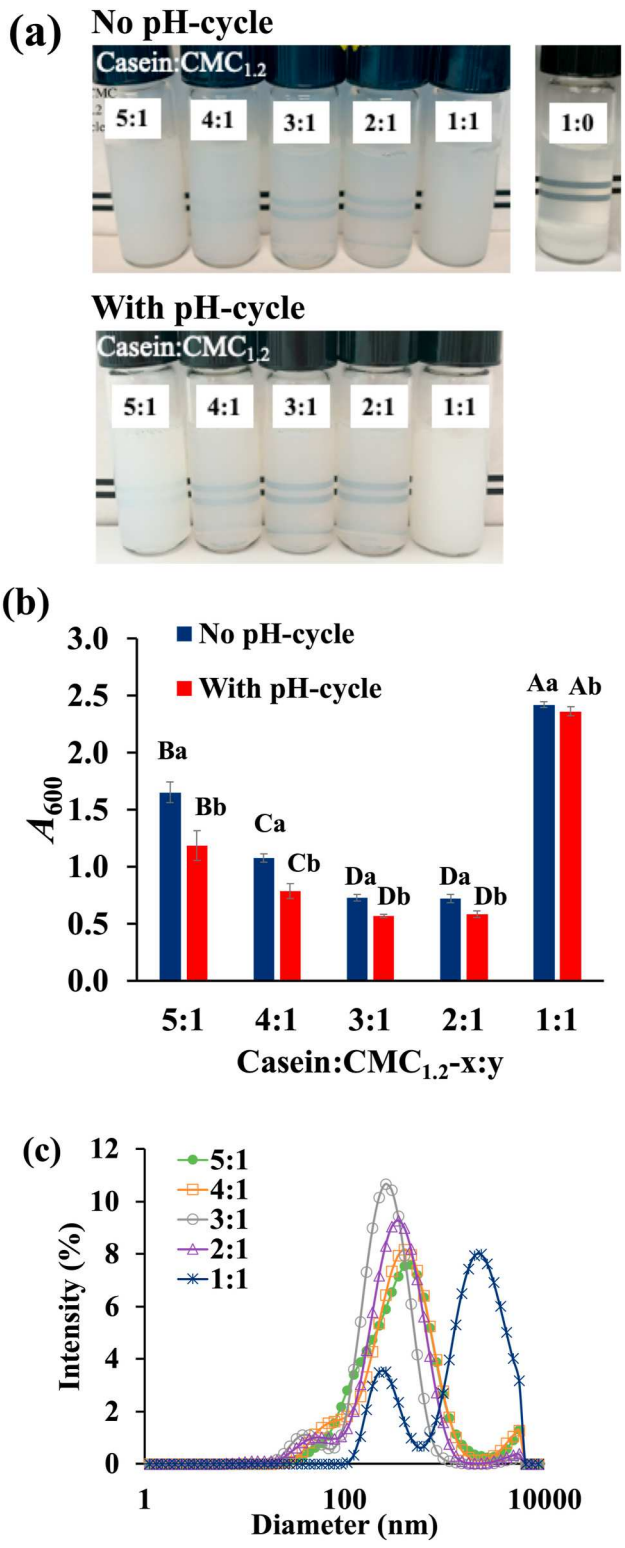

Fig. 1. Visual appearance (a) and absorbance at 600 nm (A_{600}) (b) of dispersions at pH 4.5 prepared with 1% w/v casein and different casein: CMC (DS = 1.2) mass ratios without and with the pH-cycle treatment. The size distribution of the dispersions at pH 4.5 after the pH-cycle treatment is shown in (c). In plot (b), error bars are SD (n = 3), different uppercase letters represent significant difference ($P < 0.05$) among dispersions with different biopolymer compositions, and different lowercase letters mean significant difference ($P < 0.05$) between the same sample with and without the pH-cycle treatment.

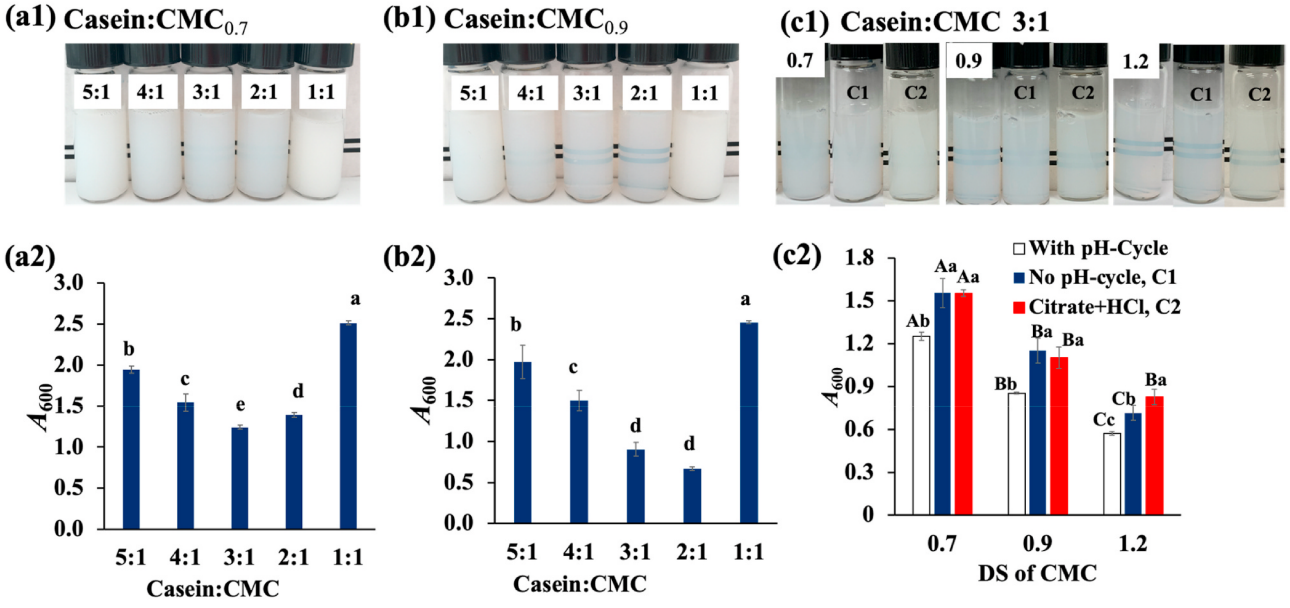

Fig. 2. Visual appearance and absorbance at 600 nm (A_{600}) of dispersions at pH 4.5, prepared with casein (1% w/v) and CMC with DS of 0.7 (a) or 0.9 (b) at different casein:CMC mass ratios using the pH-cycle treatment. Figure (c) compares pH 4.5 dispersions with casein (1% w/v) and CMC having the DS of 0.7, 0.9, and 1.2 at a constant casein:CMC mass ratio of 3:1 after the pH-cycle treatment, direct acidification from neutral pH using citric acid (labeled as "C1"), or with the same concentration of citrate as the pH-cycle treated sample but using HCl for direct acidification from neutral pH (labeled as "C2"). Error bars are SD (n = 3). Different letters in plots (a) and (b) mean significant difference among all treatments ($P < 0.05$). In plot (c), different uppercase letters represent significant difference ($P < 0.05$) among dispersions with different types of CMC, and different lowercase letters mean significant difference ($P < 0.05$) between the same sample after different treatments.

adjuster (ISA) containing KCl (Mettler-Toledo Inc., Schwerzenbach, Switzerland) was added and the ionic calcium concentration was measured using a perfectIONTM Combination Calcium Electrode (Mettler-Toledo Inc., Schwerzenbach, Switzerland) adapted to a pH meter in the electrical potential mode. Two minutes were required to reach stable readings and the Ca^{2+} concentration was calculated according to the linear relationship ($R^2 = 0.9999$) between the electrical potential (mV) and the logarithm of Ca^{2+} concentration. The free Ca^{2+} concentrations in 1% w/v casein dispersion without CMC and with 0.33% w/v CMC (casein:CMC mass ratio = 3:1) at pH 7.6 (neutral-1) and 4.5 were also measured.

2.2.5. Biopolymer interaction studied with absorption spectrum of MB

The method of Khalesi, Emadzadeh, Kadkhodaee, and Fang (2016) was adopted to study casein-CMC interactions, with some modifications. MB is a cationic dye with the maximum absorption at 664 nm and the binding with anionic polysaccharides lowers the absorption intensity centered at 664 nm (Khalesi et al., 2016; Yang, Anvari, Pan, & Chung, 2012). When MB initially binding with anionic polysaccharides is replaced by other cationic molecules, the increase of free MB molecules results in the increased absorption at 664 nm. Changes in the absorption spectra of MB therefore can be used to study the interaction mechanism between biopolymers. Experimentally, the MB stock solution was prepared at 0.1% w/v in deionized water. Then 10 μL of the MB stock solution alone or with additional 10 μL of casein/CMC [3:1] dispersion or 0.33% w/v CMC solution at pH 7.6 or pH 4.5 treated with the pH-cycle was mixed with 1 mL deionized water preadjusted to the same pH. The absorption spectra of MB were measured using the UV–vis spectrophotometer mentioned above.

2.2.6. Effects of ionic strength on the complex dimension

The impacts of electrostatic interactions on complex structure were studied for different ionic strengths (Ding, Huang, Cai, & Wang, 2019). Experimentally, NaCl was added at concentrations of 50–200 mM into casein/CMC [3:1] dispersions after 1-h incubation at pH 11.3. After the pH was decreased to 4.5, corresponding NaCl solutions at pH 4.5 were used to dilute samples, and particle size distributions were measured as described above. The particle size distribution of CMC solutions at pH 4.5, as well as that containing the highest concentration of NaCl corresponding to visually stable casein/CMC [3:1] dispersions, was also measured.

2.2.7. Statistical analysis

SSPS22.0 for Mac (SSPS Inc., Chicago, IL) was used to perform statistical analyses on values from at least duplicate experiments. Mean values were compared by one-way analysis of variance using the Tukey's test and the differences were accepted at the significance level of 0.05.

3. Results and discussion

3.1. Visual appearance and turbidity of dispersions at pH 4.5

The influence of $CMC_{1.2}$ on the stability and turbidity of micellar casein dispersions was firstly studied. Without CMC, the 1% w/v micellar casein dispersion at pH 4.5 had evident precipitation (Fig. 1a) after 1 h of the preparation. After addition of $CMC_{1.2}$, the stability of all the casein dispersions was improved, and the casein/$CMC_{1.2}$ [3:1] and casein/$CMC_{1.2}$ [2:1] samples were translucent. Except the casein/$CMC_{1.2}$ [1:1] samples, the pH-cycle treatment improved the dispersion clarity. In addition, the dispersion clarity was improved when the mass ratio of casein to CMC changed from 5:1 to 2:1 for treatments with and without the pH-cycle. Turbidity results (Fig. 1b) agreed with the visual appearance. The turbidity was decreased after the pH-cycle treatment for all the samples, which should at least be partly attributed to the smaller particles formed during acidification with citric acid following the alkalization (Pan & Zhong, 2013). Additionally, the turbidity of dispersions decreased as the casein:$CMC_{1.2}$-mass ratio decreased from 5:1 to 2:1, before a drastic increase at the mass ratio of 1:1. At a smaller casein:CMC mass ratio, more CMC molecules are available to form complexes with caseins and therefore prevent the aggregation. The lowered possibility of casein aggregation can also result from the

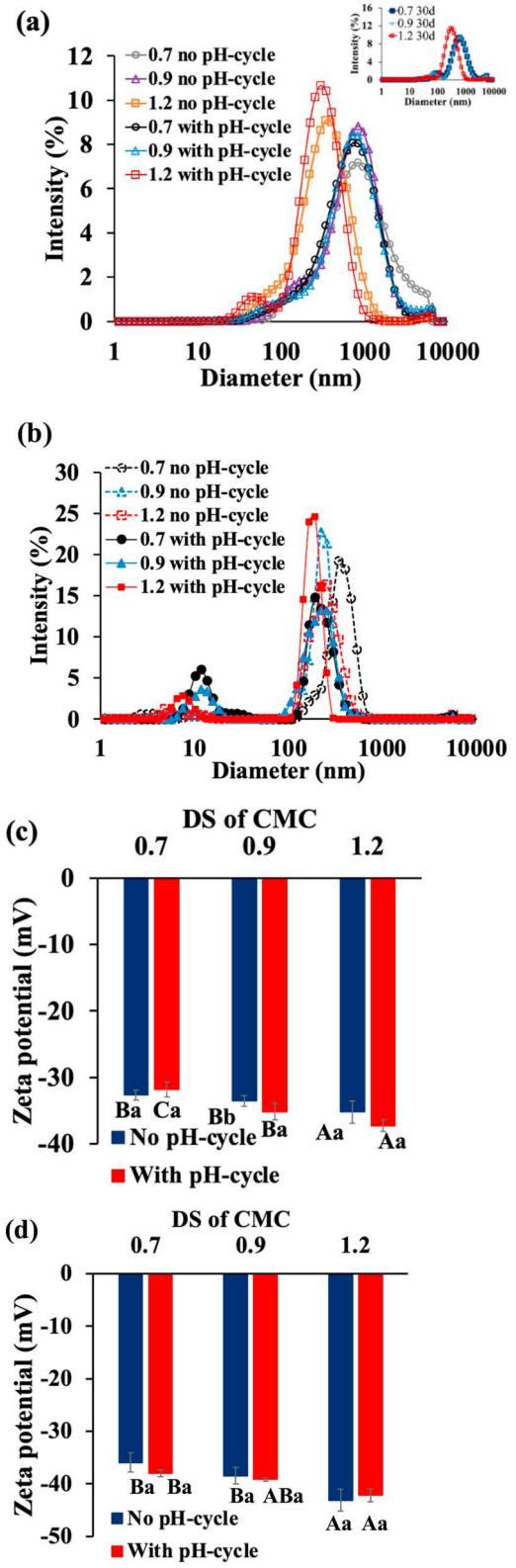

Fig. 3. The particle size distribution (a, b) and zeta potential (c, d) of CMC (b, d) or casein/CMC [3:1] (a, c) dispersions at pH 4.5. The dispersions were prepared with and without the pH-cycle treatment using CMC with a DS of 0.7, 0.9 and 1.2. The inset in (a) shows the casein/CMC [3:1] dispersions after the pH-cycle treatment and ambient storage for 30 d. In plots (c) and (d), error bars are SD (n = 3), different uppercase letters represent significant difference ($P < 0.05$) among samples with different types of CMC, and different lowercase letters mean significant difference ($P < 0.05$) between the same sample with and without the pH-cycle treatment.

increased viscosity due to a greater amount of CMC lowering the diffusion coefficient and collision of caseins and complexes (Li, Bhattacharjee, & Ghoshal, 2015; Walstra, 2002). However, depletion flocculation could cause bigger biopolymer complex particles to aggregate when CMC concentration is sufficiently high, which can explain the high turbidity of the casein/$CMC_{1.2}$ [1:1] dispersions (Corredig, Sharafbafi, & Kristo, 2011). The appearance and turbidity results were in agreement with the hydrodynamic diameter data showing the initial shift to smaller values before significant increases as the amount of CMC increased (Fig. 1c). The major peak of large particles over 1 μm for the casein/$CMC_{1.2}$ [1:1] dispersion indicates the depletion flocculation-induced aggregation.

Similar trends were observed for the mixture dispersions prepared with casein and $CMC_{0.7}$ or $CMC_{0.9}$ following the pH-cycle treatment (Fig. 2a and b). Dispersions with the casein:CMC mass ratio of 3:1 had the lowest turbidity for all three kinds of CMC, and therefore this mass ratio was used for further study. For casein/CMC [3:1] samples, the turbidity decreased as the charge density of CMC increased (Fig. 2c). CMC with a higher charge density has a greater tendency and capacity to bind with caseins (Xiong et al., 2017). Additionally, CMC chains with a higher charge density are more stretched due to the enhanced intramolecular repulsions, and can provide stronger electrostatic and steric repulsions when present on the surface of casein-CMC complexes (Wang, Pillai, & Nickerson, 2019; Xiong, Ren, Li, & Li, 2018).

The control samples of casein/CMC [3:1] without the pH-cycle treatment had higher turbidity than the corresponding dispersions treated with the pH-cycle (Fig. 2c). During the pH-cycle treatment, about 8.5 mM citric acid was added and the citrate ions may also bind calcium ions to affect the reassociation of dissociated caseins during acidification from pH 11.3 to 4.5. To confirm that the reduced turbidity of dispersions was not contributed by the chelating property of citrate ions alone, sodium citrate was added at 8.5 mM after hydrating casein and CMC at neutral pH, and then HCl was used to decrease the pH to 4.5. The A_{600} of pH 4.5 casein/CMC [3:1] dispersions as prepared was 1.56, 1.10, and 0.83, respectively, for treatments with $CMC_{0.7}$, $CMC_{0.9}$, and $CMC_{1.2}$, which was all higher than the corresponding pH-cycle treated samples (Fig. 2c), indicating that the pH-cycle was necessary to further improve dispersion clarity. The A_{600} of pH 4.5 casein/CMC [3:1] dispersions as prepared was similar ($P > 0.05$) to the corresponding sample without the pH-cycle treatment (direct acidification from neutral pH to pH 4.5 with citric acid) for the $CMC_{0.7}$ and $CMC_{0.9}$ treatments but was higher for the $CMC_{1.2}$ treatment. These comparisons indicate the contribution of citrate to turbidity reduction of the mixture dispersions after acidification to pH 4.5.

3.2. Particle size and ζ-potential of dispersions at pH 4.5

Without the pH-cycle treatment, the casein/CMC [3:1] dispersions at pH 4.5 shifted to smaller particles as the charge density of CMC increased (Fig. 3a), which was in agreement with the turbidity data in Fig. 2c. After being treated with the pH-cycle, the hydrodynamic diameter at pH 4.5 was further reduced for all samples, and the casein/$CMC_{1.2}$ [3:1] had the smallest particles (Fig. 3a), corresponding to the lowest turbidity (Fig. 2). After storage at RT for 30 days, particle size distributions of all the dispersions treated with the pH-cycle had unnoticeable changes (Fig. 3a inset), indicating good stability of all the samples.

The particle size distributions of CMC at pH 4.5 are shown in Fig. 3b. When compared to direct acidification (no pH-cycle), particle size distributions of all CMC samples shifted to a smaller region after the pH-cycle treatment. At alkaline pH, CMC is more extensively charged to cause the enhanced disentanglement of CMC molecules, which leads to a higher content of disentangled/hydrated CMC after acidification to pH 4.5. When comparing to casein/CMC dispersions (Fig. 3a), it can be deduced that complexes had a larger hydrodynamic diameter than CMC.

All the dispersions had a negative ζ-potential (Fig. 3c). Because

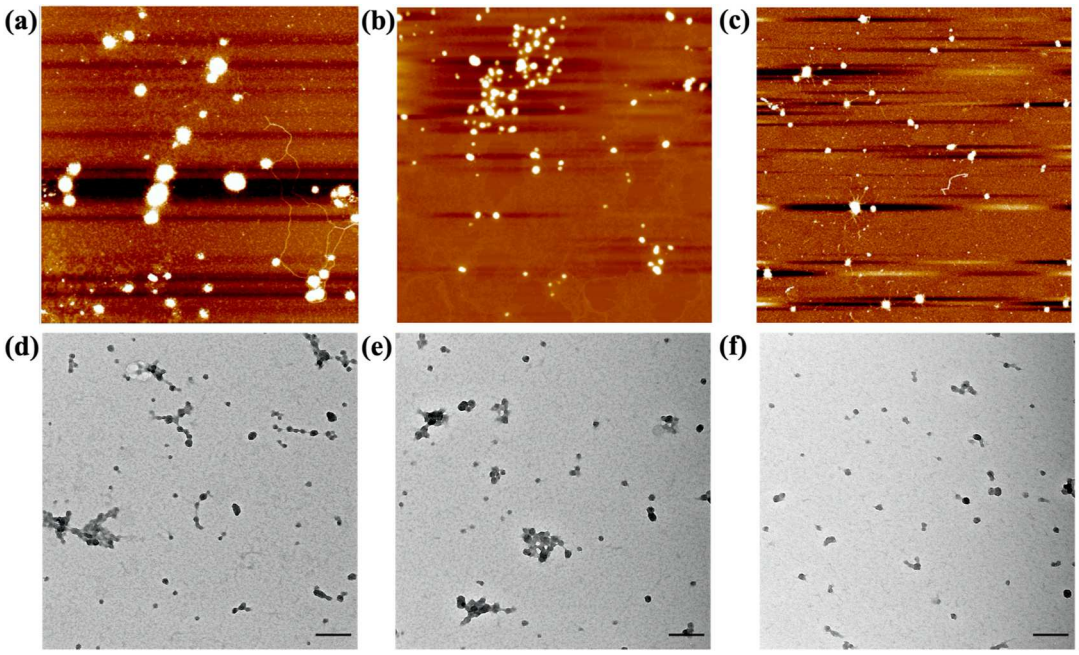

Fig. 4. AFM (5 × 5 μm) (a–c) and TEM (d–f) images of pH 4.5 dispersions prepared with the pH-cycle treatment using casein/CMC at a mass ratio of 3:1 and DS of CMC being 0.7 (left), 0.9 (center), and 1.2 (right). Scale bar = 200 nm in (d–f).

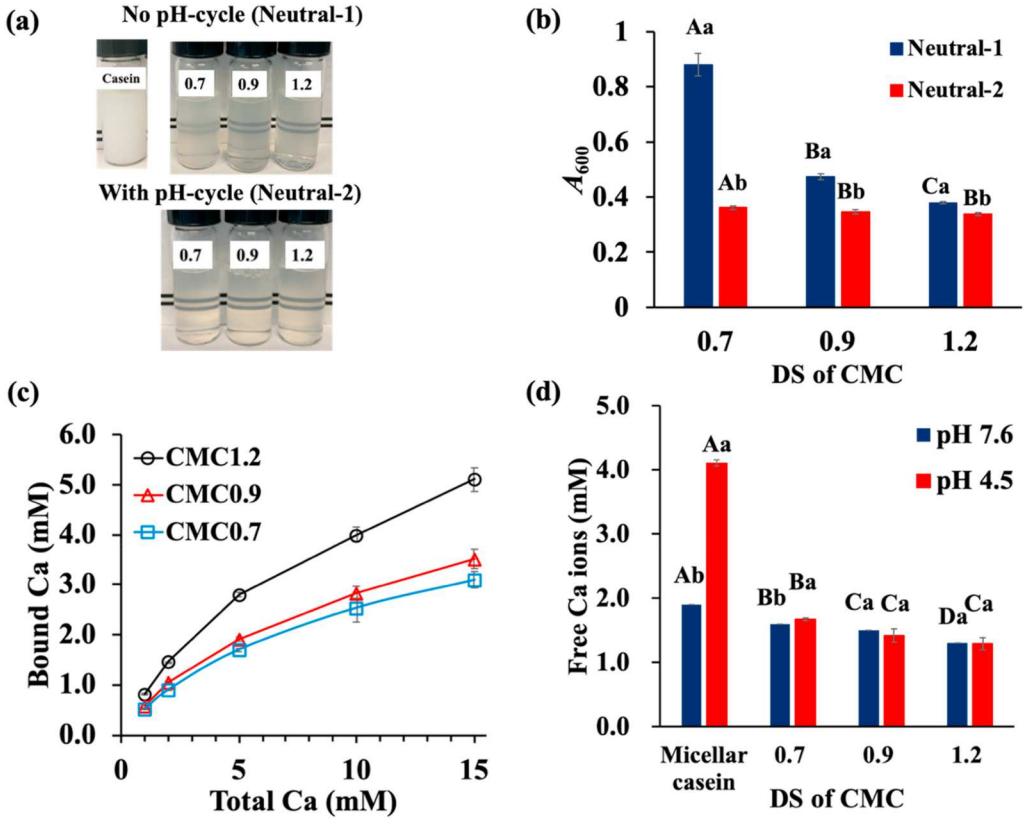

Fig. 5. Visual appearance (a) and absorbance at 600 nm (A_{600}, b) of pH 7.6 dispersions with micellar caseins or casein/CMC mixture with a mass ratio of 3:1 and the DS of CMC being 0.7, 0.9 or 1.2, prepared without pH adjustment (neutral 1) or with the pH-cycle treatment (neutral 2). Calcium-chelating properties measured as the bound Ca^{2+} concentration in solutions with 0.33% w/v CMC and different initial $CaCl_2$ concentrations are shown in (c), while free Ca^{2+} concentrations in micellar casein and casein/CMC dispersions after overnight (about 15 h) hydration and at pH 4.5 with the pH-cycle treatment are shown in (d). Different uppercase and lowercase letters in plots (b) and (d) compare treatments as shown on the X-axis and the legend, respectively. Error bars are SD (n = 3).

caseins have a net charge of close to zero at pH 4.5, the negative charges should originate from CMC on the surface of casein particles (Sejersen et al., 2007). The ζ-potential of CMC is shown in Fig. 3d. CMC molecules are negatively charged at pH 4.5, as expected, due to carboxyl groups with the pKa of 3.5 (Harnsilawat et al., 2006). The larger magnitude of ζ-potential with the increased DS of CMC confirms the higher charge density. Colloidal particles with the ζ-potential magnitude of over 30 mV are recognized as stable against aggregation due to electrostatic repulsion (Patel & Agrawal, 2011). Therefore, electrostatic repulsion alone may be sufficient to prevent the aggregation of nanocomplexes. The stability of nanocomplexes is further strengthened by steric repulsion originating from biopolymers on the particle surface (Patel &

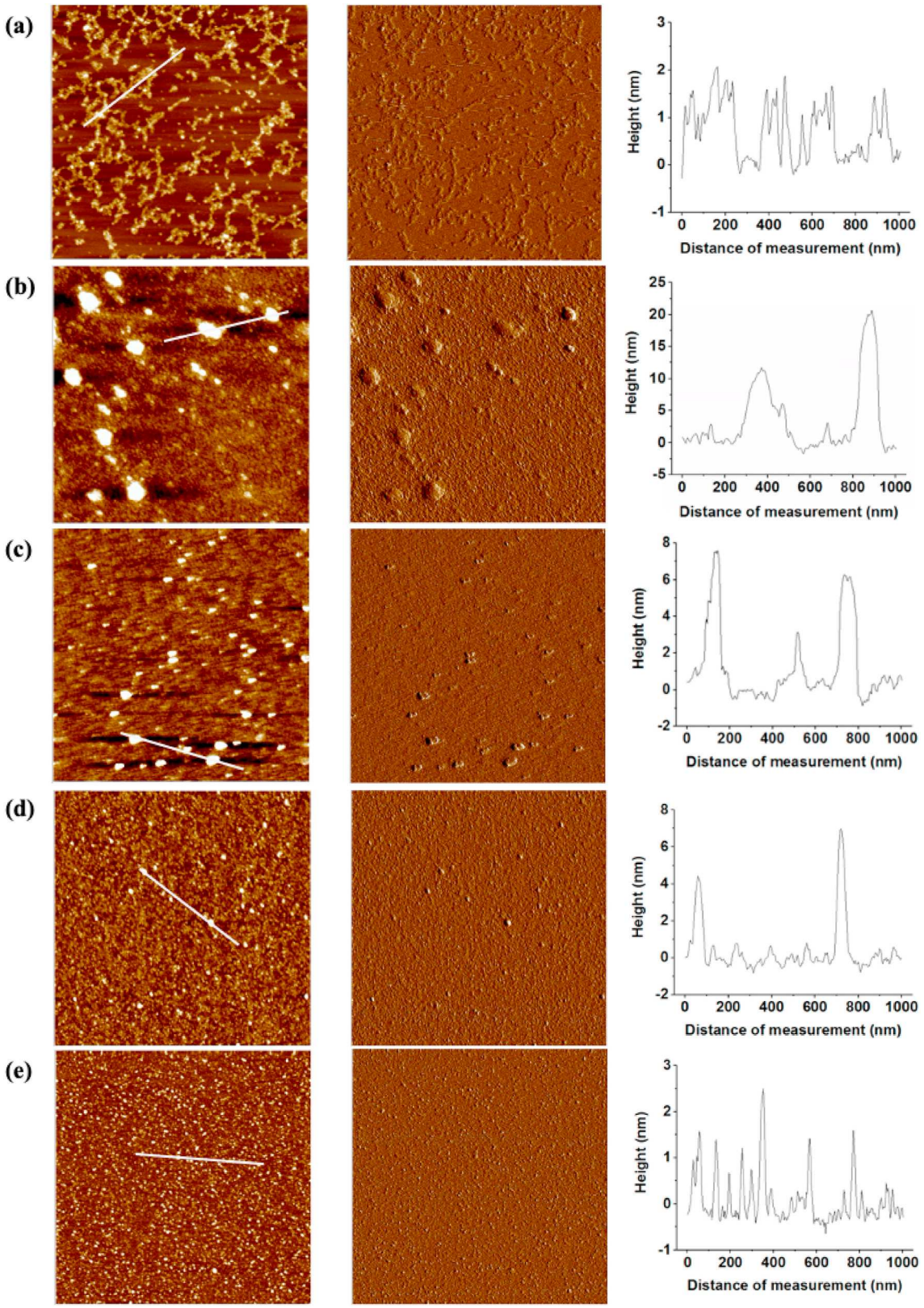

Fig. 6. AFM images (2 × 2 μm) in height (left) and peak force error (middle) modulus channels showing CMC with a DS of 1.2 (a), micellar casein (b), and casein/CMC mixtures prepared at a mass ratio of 3:1 and DS of CMC being 0.7 (c), 0.9 (d), and 1.2 (e). Dispersions were prepared at neutral pH without the pH-cycle treatment. Plots (right) show the height distribution of particles along the white line.

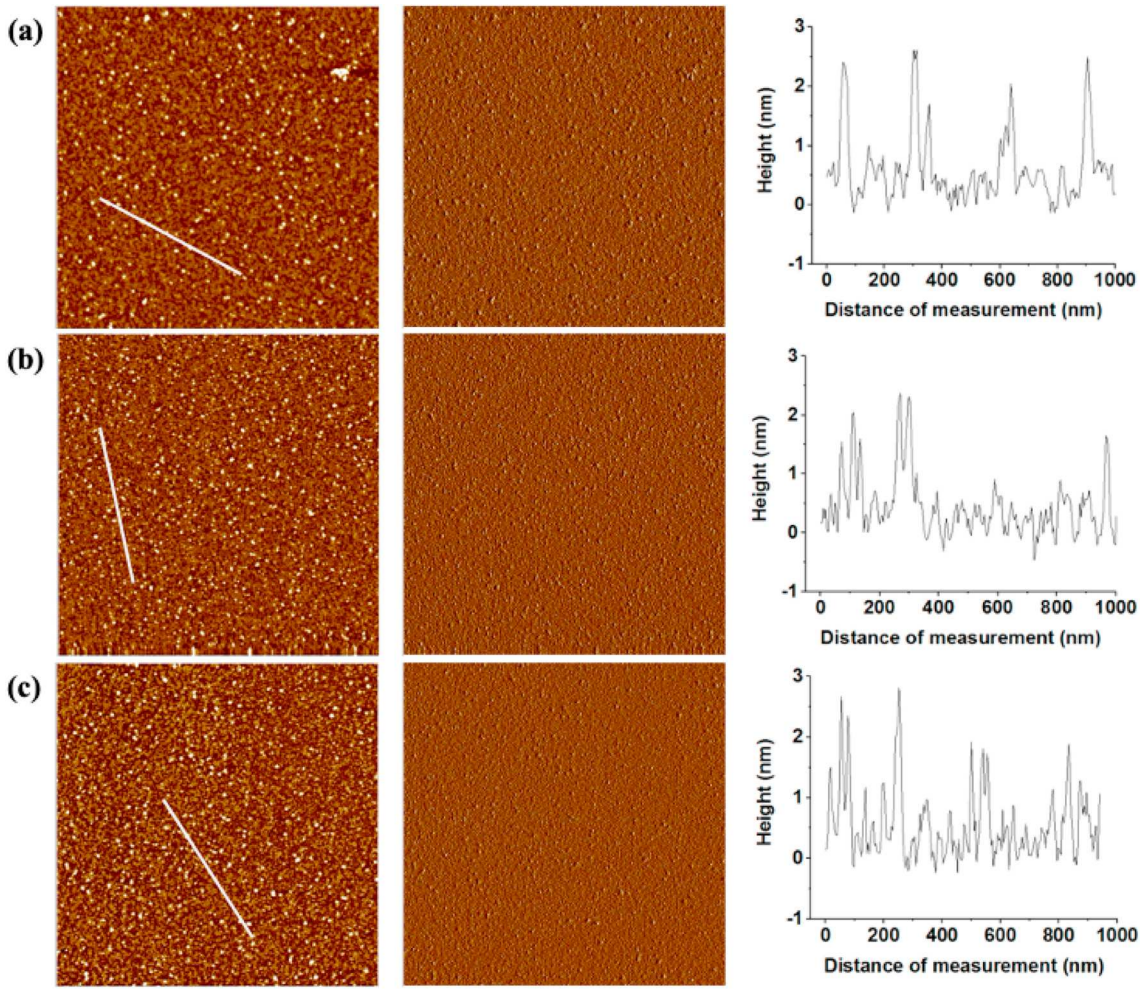

Fig. 7. AFM images (2 × 2 μm) in height (left) and peak force error (middle) modulus channels showing neutral dispersions with casein and CMC at a mass ratio of 3:1 using CMC at a DS of 0.7 (a), 0.9 (b), and 1.2 (c) and following the pH-cycle treatment. Plots (right) show the height distribution of particles along the white line.

Agrawal, 2011). Additionally, the viscosity is increased by possible free CMC molecules, more significant at a higher charge density, to enhance particle stability (Du et al., 2009). All these three factors can contribute to the high stability of casein/CMC dispersions, as shown in Fig. 3a.

3.3. Morphology of complexes at pH 4.5

The AFM morphology of casein/CMC [3:1] complexes at pH 4.5 after the pH-cycle treatment is shown in Fig. 4. Some of the complexes appeared as discrete mostly spherical particles, and some had irregular shapes consisting of associated particles. The casein/$CMC_{0.7}$ [3:1] complexes had the largest diameter, and some particles appeared to be bridged by polysaccharide chains. As the DS of CMC increased, smaller particles were observed, and the particle association became less, which agree with the reduced hydrodynamic diameter (Fig. 3) and turbidity (Fig. 2). Additional TEM analysis (Fig. 3) confirmed the trend observed in AFM. Overall, the casein/$CMC_{1.2}$ [3:1] complexes were well dispersed and had the smallest dimension.

3.4. Calcium-binding properties of CMC

After the overnight hydration, the clarity of neutral casein/CMC [3:1] dispersions was drastically improved when compared with the micellar casein only dispersion, and the turbidity was lower at a higher charge density of CMC (Fig. 5a). The carboxylate groups of CMC have a potential to bind calcium ions, which drives the calcium balance from casein micelles to the serum phase to dissociate and/or loosen casein micelles, resulting in the reduced turbidity (Pitkowski, Nicolai, & Durand, 2008). The further reduction of turbidity after increasing pH to 11.3 and reducing to neutral pH (Fig. 5b) should be contributed to the complete disassociation of casein micelles at alkaline conditions and the formation of smaller particles during the following acidification (Pan & Zhong, 2013).

To directly study the calcium chelation properties of CMC, the concentration of bound calcium ions in 0.33% w/v CMC solutions mixed with different $CaCl_2$ concentrations at neutral pH was determined (Fig. 5c). As the charge density of CMC increased, the amount of bound calcium ions increased, which is expected because more carboxylate groups at a higher charge density provide more sites to bind with calcium ions. The concentrations of free calcium ions in micellar casein and casein/CMC dispersions at neutral pH and pH 4.5 were also determined (Fig. 5d). More calcium ions were released in micellar casein dispersions at pH 4.5 than at neutral pH because the hydration and dissolution of colloidal calcium phosphate are favored at acidic pH (Orlien, Boserup, & Olsen, 2010). In casein/CMC dispersions, the concentration of free calcium ions was significantly lower ($p < 0.05$) than that of micellar casein dispersions and significantly decreased with an increase in the charge density of CMC; however, the significantly higher calcium ion concentration at pH 4.5 than at neutral pH was only observed for the $CMC_{0.7}$ treatment. Therefore, chelating properties of CMC as determined using $CaCl_2$ solutions also were critical to ionic and complexation properties of casein/CMC dispersions.

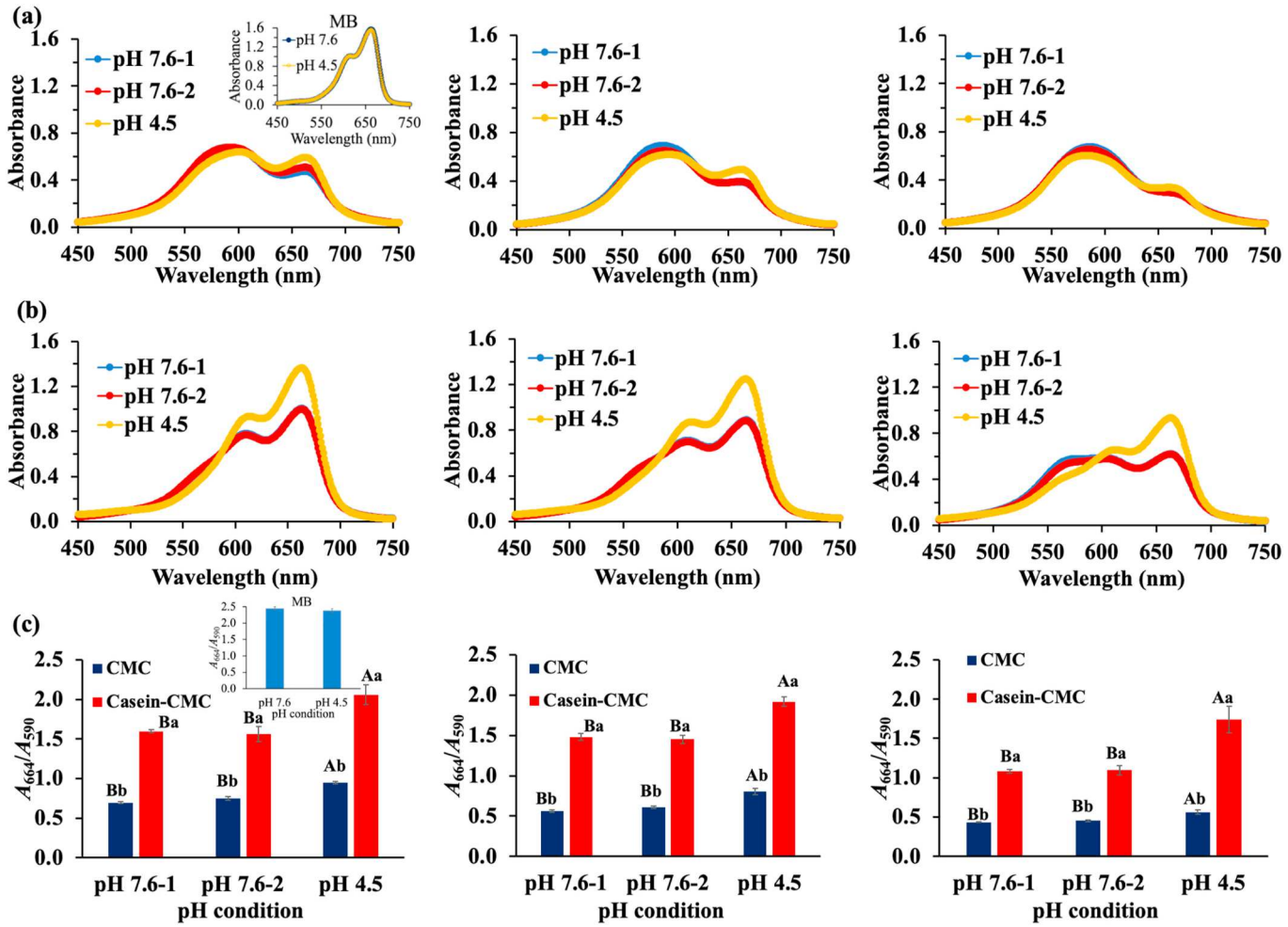

Fig. 8. Absorption spectra of methylene blue (MB) in CMC solutions (a) and casein/CMC [3:1] dispersions (b). Plot (c) compares the A_{664}/A_{590} value calculated from the results of (a)&(b). Plots from left to right represent samples containing CMC with the DS of 0.7, 0.9 and 1.2, respectively. The insets in (a) and (c) show the results of MB in water. The pH 7.6–1 and 7.6–2 mean samples at pH 7.6 prepared without pH adjustment or with the pH-cycle treatment, respectively. The pH 4.5 samples are treated with the pH-cycle. Different uppercase and lowercase letters in plot (c) compare treatments as shown on the X-axis and the legend, respectively. Error bars are SD (n = 2).

To further understand chelating properties of CMC, the morphology of biopolymer structures was studied using AFM. Fig. 6 presents the morphology of $CMC_{1.2}$, micellar casein, and casein/CMC dispersions at neutral pH without the pH-cycle treatment. As a representative of CMC, $CMC_{1.2}$ had polymeric structures with a height of no more than 3 nm, which suggests a relatively low mass density at neutral pH. Micellar casein appeared as compact particulates and had a relatively high mass density indicated by the height of up to 20 nm. After thoroughly mixing casein micelles with CMC, the diameter of particulates and the mass density both decreased (Fig. 6c–e). The diameter and mass density of the biopolymer mixtures were decreased to a higher degree as the charge density of CMC increased, indicating a greater extent of casein micelle dissociation. After the pH-cycle treatment, all the casein/CMC dispersions at neutral pH had small particles with a low mass density (Fig. 7), suggesting that casein micelles were dissociated during alkalization and the reassociation of casein during the subsequent acidification step was limited. The morphology similarity of casein/CMC dispersions with different types of CMC at neutral pH (Fig. 7) contrasts with the difference of casein-CMC complexes at pH 4.5 (Fig. 4), suggesting that charge density of CMC is critical to the complexation of casein and CMC at acidic conditions. Overall, the particle morphology characterized using AFM agrees with the visual appearance and turbidity changes of dispersions before and after the pH-cycle treatment (Fig. 5a&b) and chelating properties of CMC (Fig. 5).

3.5. Interaction between caseins and CMC studied with absorption spectra of MB

The absorption spectra of MB were used to study the interaction between casein and CMC at neutral pH and pH 4.5. As shown in Fig. 8a inset, free MB molecules are characterized by a maximum absorption at 664 nm with a shoulder around 610 nm (Tafulo, Queirós, & González-Aguilar, 2009). The interaction between MB and anionic polysaccharides through electrostatic interactions induces the decreased intensity of absorption peak at 664 nm, along with a shift to shorter wavelengths (blue shift) (Khalesi et al., 2016). After mixing with CMC, the peak intensity at 664 nm was greatly decreased and the major peak shifted to around 590 nm (Fig. 8a), indicating the binding of MB to CMC. In casein/CMC [3:1] dispersions, the shape of spectra was more similar to that of free MB (Fig. 8b) at both pH 7.6 and 4.5 than the mixtures of MB and CMC, with the increased and decreased peak intensity around 664 and 590 nm, respectively, which indicates the increased amount of free MB molecules due to complex formation between casein and CMC (Rohart, Bouveresse, Rutledge, & Michon, 2015). Additionally, the ratio of absorbance at 664 nm and that at 590 nm (A_{664}/A_{590}) was used to analyze the relative abundance of free MB molecules (Fig. 8c) (Khalesi et al., 2016). MB itself (Fig. 8c inset) had the highest A_{664}/A_{590} value ($P < 0.05$), suggesting the binding of MB to biopolymers in all other samples. For all three types of CMC, the A_{664}/A_{590} value of casein/CMC

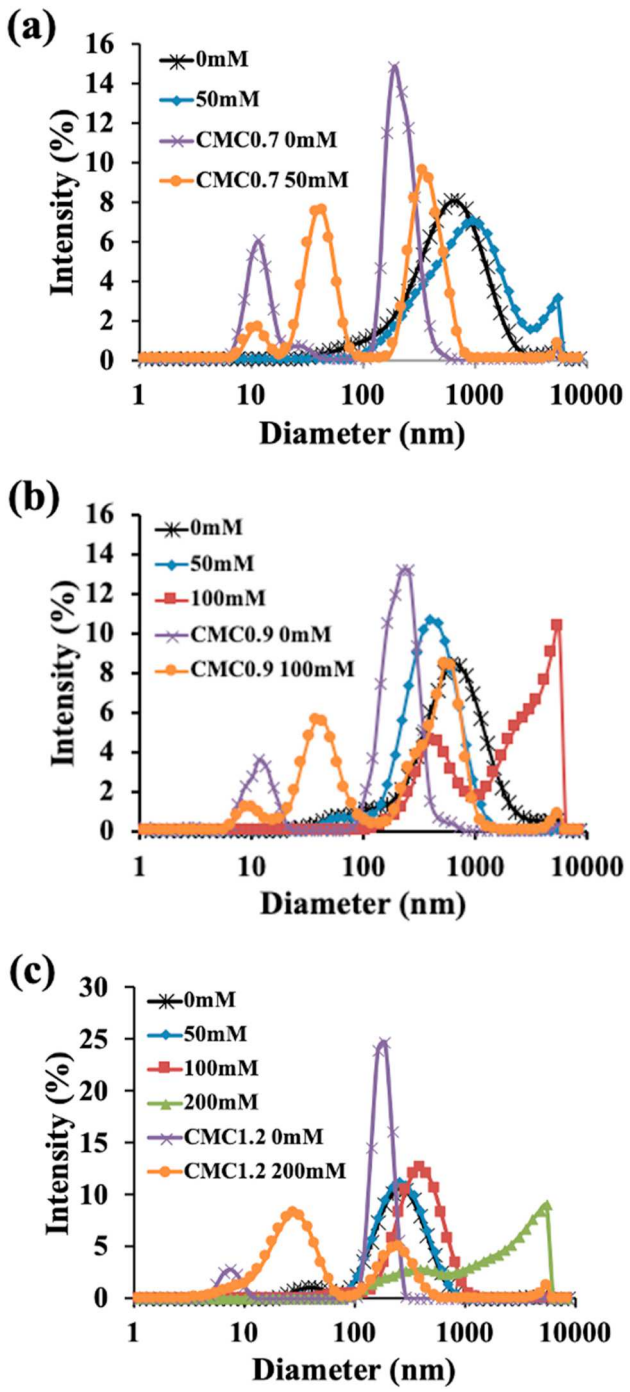

Fig. 9. Influence of 0–200 mM NaCl on the particle size distribution of pH 4.5 dispersions with 1% w/w casein and CMC at a casein:CMC mass ratio of 3:1 and CMC DS of 0.7 (a), 0.9 (b) or 1.2 (c), following the pH-cycle treatment. Dispersions with 100 and 200 mM NaCl in (a) and 200 mM NaCl in (b) were not measured due to precipitation. The particle size distributions of CMC at 0 mM and the highest concentration of NaCl enabling stable casein dispersions are also presented for reference.

dispersions was higher than that of CMC solutions, and the difference was more significant at pH 4.5 than pH 7.6. The data in Fig. 8 indicate the presence of more free MB molecules in casein/CMC dispersions than CMC solutions, as well as more free MB molecules at pH 4.5 than pH 7.6 in both CMC and casein/CMC dispersions (Rohart et al., 2015). The latter is expected as the amount of negative charges is smaller at a lower pH for both casein and CMC. The former indicates the impact of casein on binding between CMC and MB.

At pH 7.6, negative charges of caseins could also bind with MB (data not shown), and the binding of MB to both CMC and caseins would result in the A_{664}/A_{590} values of the casein/CMC mixture being smaller than that of the corresponding CMC. However, the A_{664}/A_{590} value of casein/CMC dispersions was higher than that of the corresponding CMC solution (Fig. 8c). This suggests that the binding between caseins and MB is negligible in casein/CMC dispersions and some negative charges of CMC are bound by caseins to reduce the total amount of bound MB. The same analogy can be applied at pH 4.5. The bigger A_{664}/A_{590} value of casein/CMC mixtures at pH 4.5 than at pH 7.6 suggests that CMC is bound with a greater amount of positive charges of caseins, which is expected as caseins have more positive charges at pH 4.5 than pH 7.6 and this is enabled by the improved flexibility of CMC due to a reduced extent of ionization at a lower pH. Although the reduced ionization also results in a significant increase of the A_{664}/A_{590} value when CMC solution pH is decreased from 7.6 to 4.5 (Fig. 8c), the greater difference between the A_{664}/A_{590} value of CMC/casein mixtures and that of CMC at pH 4.5 than at pH 7.5 suggests the enhanced effect of caseins binding with CMC at pH 4.5.

Results in Fig. 8 confirm that the electrostatic attraction between CMC and caseins occurs at both pH 7.6 and 4.5 and is stronger at pH 4.5. Additionally, the A_{664}/A_{590} values at pH 4.5 show significant differences between CMC and the complex dispersions, which was not the case for the magnitude difference of their ζ-potentials (Fig. 3c&d). The ζ-potential is determined based on the electrophoretic mobility of overall particles and is not identical to the surface charge (Bhattacharjee, 2016). Results in Fig. 8 suggest MB spectra can be used as a more sensitive technique to study interactions and charge characteristics of polyelectrolyte complexes.

3.6. The stability of casein-CMC complexes at increased ionic strength

Because electrostatic attraction is the major force for the complexation between casein and CMC, increases in the ionic strength are expected to destabilize the system by screening effective surface charges on polyelectrolytes (Huang, Sun, Xiao, & Yang, 2012). The particle size distribution of casein/CMC dispersions after the addition of NaCl is shown in Fig. 9, with reference to that of CMC. In the casein/$CMC_{0.7}$ [3:1] dispersion, particles shifted to larger sizes at 50 mM NaCl, and a new peak over 1000 nm indicates the aggregation of particles. In addition, precipitation occurred when NaCl was increased to 100 mM. It is possible that complex structures became loosened and/or casein was partially detached to cause aggregation of complexes at 50 mM NaCl, both of which can increase the measured hydrodynamic diameter. At 100 mM, the strong charge screening effect caused a high extent of casein detachment and therefore precipitation. The casein/$CMC_{0.9}$ [3:1] sample shifted to smaller sizes at 50 mM NaCl, which indicates the absence of casein detachment and can be attributed to the weakened electrostatic repulsion between ionized segments within complexes as well as the less extended CMC chain on complex surface. The hydrodynamic diameters and polydispersity greatly increased when the NaCl concentration of casein/$CMC_{0.9}$ [3:1] sample reached 100 mM, which is similar to the casein/$CMC_{0.7}$ [3:1] sample with 50 mM NaCl, except with the greater resistance to structural changes due to the increased charge density/binding strength of CMC. For casein dispersions containing $CMC_{1.2}$, particle sizes were stable at 50 and 100 mM of NaCl, showing only one peak, and the diameter increase was observed at a higher NaCl concentration of 200 mM. These data confirm the significance of electrostatic attraction between casein and CMC during the complexation, and also indicate that a higher charge density of CMC results in stronger intermolecular electrostatic attraction within complexes to become more resistant to charge screening at an increased ionic strength. As food products are complex systems that may contain various ingredients including many salts, the ability to manipulate properties of casein/CMC complexes by controlling the DS of CMC provides great flexibility in

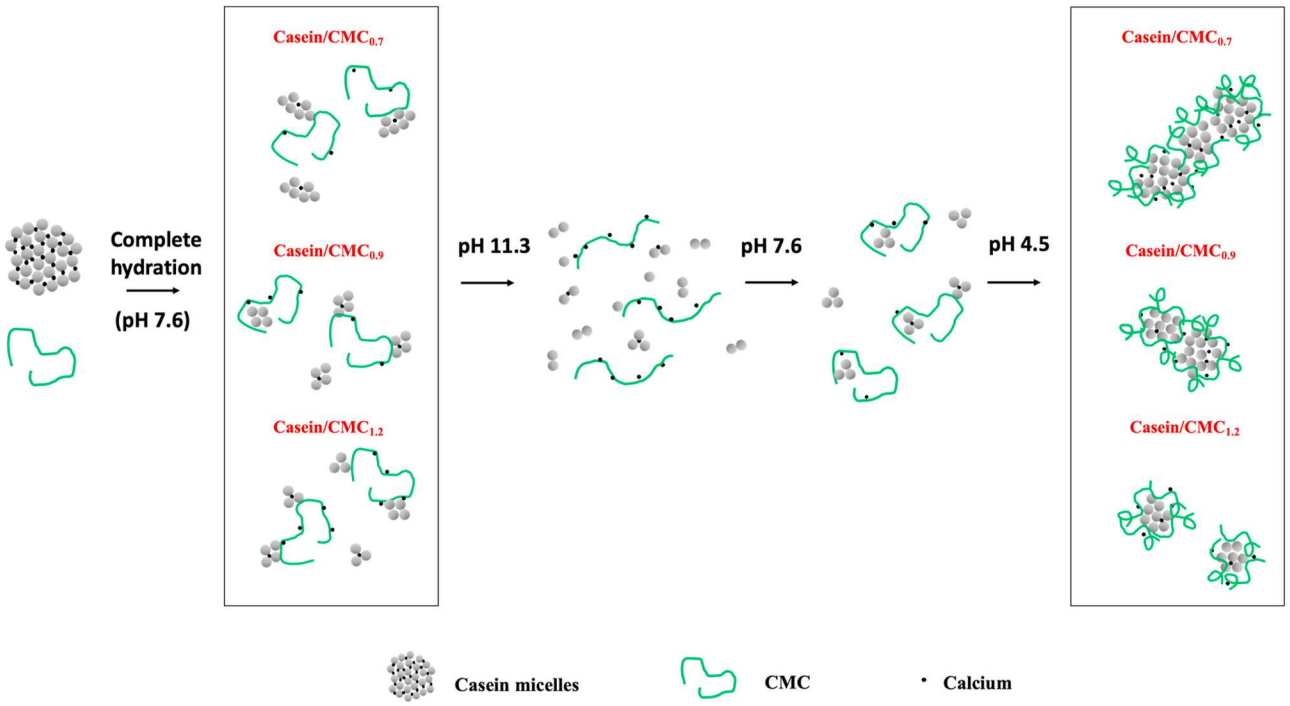

Fig. 10. Possible structural changes of casein and CMC following the pH-cycle treatment as affected by the DS of CMC.

formulations.

3.7. Possible mechanism of complex formation

Possible complex formation mechanisms are proposed based on the cumulative evidences from various techniques, shown in Fig. 10. After the thorough mixing of casein micelles and CMC, some calcium ions are chelated from casein micelles by CMC, resulting in the disassociation of casein micelles, with a higher degree at a higher charge density of CMC (Fig. 6). During the pH-cycle treatment, casein micelles are completely disassociated and CMC is highly stretched when the dispersions are alkalized to pH 11.3. After the following acidification to neutral pH, caseins are still mostly dissociated as indicated by the AFM images (Fig. 7), and there is a limited extent of electrostatic binding between positively charged patches of casein and CMC at neutral pH (Fig. 8), as reported for other protein-polysaccharide systems when both biopolymers are overall negatively charged (Khalesi et al., 2016; Rohart et al., 2015). The strong electrostatic and steric repulsions prevent the extensive reassociation of caseins at neutral pH. When pH is continuously decreased to 4.5, casein become more positively charged to promote the binding with CMC. At the same time, caseins are pulled toward each other due to hydrophobic attraction to form particulates, orienting hydrophilic CMC on the surface and leading to a casein core – CMC shell structure. This structure is supported by the similar ζ-potential of the complexes and the corresponding CMC (Fig. 3). CMC on the complex surface helps to prevent the further aggregation of caseins due to the electrostatic and steric repulsions. CMC with a higher charge density is more stretched because of the stronger intramolecular repulsion, and therefore is able to provide more sites to bind with caseins (Wang, Pillai, & Nickerson, 2019; Xiong et al., 2017). This higher binding capacity and the stronger electrostatic attraction between casein and CMC result in smaller and more stable complexes at a higher DS of CMC (Fig. 4) (Xiong et al., 2018).

In the mixture dispersions without the pH-cycle treatment, the complexation mechanisms should be similar. However, larger particles are formed because casein micelles are only partially disassociated at neutral pH before dispersions are directly acidified (Fig. 3). The greater capacity of CMC chelating calcium at a higher DS (Fig. 5) results in a higher extent of casein micelle dissociation and therefore smaller complexes and lower dispersion turbidity.

4. Conclusions

CMC with different charge densities improved the stability and clarity of casein dispersions at pH 4.5 without and with the pH-cycle treatment. CMC was capable of chelating calcium from casein micelles to result in partial dissociation and the chelating capacity increased as the charge density of CMC increased. The resultant casein/CMC dispersion had a lower turbidity than casein dispersions, and the dispersion turbidity was further reduced by the pH-cycle treatment. During the pH-cycle treatment, casein micelles were completely disassociated at alkaline conditions, enabling the formation of small complexes with CMC during the following acidification through electrostatic attraction between casein and CMC and hydrophobic attraction between caseins. The orientation of CMC on complex surfaces, either with or without the pH-cycle treatment, prevented casein aggregation and improved dispersion clarity at pH 4.5. Lowering dispersion turbidity was additionally enabled by increasing the charge density of CMC. This study may be significant to the application of casein-containing ingredients in the production of acidic beverages. Additionally, findings from this study may be meaningful to broaden the application of carboxylated polysaccharides by utilizing their combined chelating and complexation properties.

CRediT authorship contribution statement

Nan Li: Conceptualization, Methodology, Formal analysis, Investigation, Writing – original draft, Visualization. **Qixin Zhong:** Conceptualization, Methodology, Resources, Writing – review & editing, Supervision, Project administration, Funding acquisition.

Declaration of competing interest

The authors declare that they have no known competing financial

interests or personal relationships that could have appeared to influence the work reported in this paper.

Acknowledgements

Funding of this work was provided by the University of Tennessee, and United States Department of Agriculture NIFA award TEN 2015-05921 and Hatch Projects TEN00487 and TEN00568. Any opinions, findings, conclusions, or recommendations expressed in this publication are those of the author(s) and do not necessarily reflect the view of the U.S. Department of Agriculture.

References

An, Y., Cui, B., Wang, Y., Jin, W., Geng, X., Yan, X., et al. (2014). Functional properties of ovalbumin glycosylated with carboxymethyl cellulose of different substitution degree. *Food Hydrocolloids, 40*, 1–8.

Bhattacharjee, S. (2016). DLS and zeta potential–what they are and what they are not? *Journal of Controlled Release, 235*, 337–351.

Cai, X., Luan, Y., Dong, Q., Shao, W., Li, Z., & Zhao, Z. (2011). Sustained release of 5-fluorouracil by incorporation into sodium carboxymethylcellulose sub-micron fibers. *International Journal of Pharmaceutics, 419*(1–2), 240–246.

Cai, Z., Wei, Y., Guo, Y., Ma, A., & Zhang, H. (2020). Influence of the degree of esterification of soluble soybean polysaccharide on the stability of acidified milk drinks. *Food Hydrocolloids, 108*, Article 106052.

Cai, Z., Wu, J., Du, B., & Zhang, H. (2018). Impact of distribution of carboxymethyl substituents in the stabilizer of carboxymethyl cellulose on the stability of acidified milk drinks. *Food Hydrocolloids, 76*, 150–157.

Claeys, W., Verraes, C., Cardoen, S., De Block, J., Huyghebaert, A., Raes, K., et al. (2014). Consumption of raw or heated milk from different species: An evaluation of the nutritional and potential health benefits. *Food Control, 42*, 188–201.

Corredig, M., Sharafbafi, N., & Kristo, E. (2011). Polysaccharide–protein interactions in dairy matrices, control and design of structures. *Food Hydrocolloids, 25*, 1833–1841.

Culler, M., Saricay, Y., & Harte, F. (2017). The effect of emulsifying salts on the turbidity of a diluted milk system with varying pH and protein concentration. *Journal of Dairy Science, 100*(6), 4241–4252.

Dalgleish, D. G. (2011). On the structural models of bovine casein micelles—review and possible improvements. *Soft Matter, 7*(6), 2265–2272.

Dalgleish, D. G., & Corredig, M. (2012). The structure of the casein micelle of milk and its changes during processing. *Annual Review of Food Science and Technology, 3*, 449–467.

Dhanasingh, S., & Nallaperumal, S. K. (2010). Chitosan/casein microparticles: Preparation, characterization and drug release studies. *International Journal of Engineering and Applied Sciences, 6*(234), 238.

Ding, L., Huang, Y., Cai, X., & Wang, S. (2019). Impact of pH, ionic strength and chitosan charge density on chitosan/casein complexation and phase behavior. *Carbohydrate Polymers, 208*, 133–141.

Du, B., Li, J., Zhang, H., Chen, P., Huang, L., & Zhou, J. (2007). The stabilization mechanism of acidified milk drinks induced by carboxymethylcellulose. *Le Lait, 87*(4–5), 287–300.

Du, B., Li, J., Zhang, H., Huang, L., Chen, P., & Zhou, J. (2009). Influence of molecular weight and degree of substitution of carboxymethylcellulose on the stability of acidified milk drinks. *Food Hydrocolloids, 23*(5), 1420–1426.

Farías, M. E., Martinez, M. J., & Pilosof, A. M. R. (2010). Casein glycomacropeptide pH-dependent self-assembly and cold gelation. *International Dairy Journal, 20*(2), 79–88.

Farrell, H., Jr., Jimenez-Flores, R., Bleck, G., Brown, E., Butler, J., Creamer, L., et al. (2004). Nomenclature of the proteins of cows' milk—sixth revision. *Journal of Dairy Science, 87*(6), 1641–1674.

Gibis, M., Schuh, V., & Weiss, J. (2015). Effects of carboxymethyl cellulose (CMC) and microcrystalline cellulose (MCC) as fat replacers on the microstructure and sensory characteristics of fried beef patties. *Food Hydrocolloids, 45*, 236–246.

Harnsilawat, T., Pongsawatmanit, R., & McClements, D. (2006). Characterization of β-lactoglobulin–sodium alginate interactions in aqueous solutions: A calorimetry, light scattering, electrophoretic mobility and solubility study. *Food Hydrocolloids, 20*(5), 577–585.

Huang, H., Belwal, T., Aalim, H., Li, L., Lin, X., Liu, S., et al. (2019). Protein-polysaccharide complex coated W/O/W emulsion as secondary microcapsule for hydrophilic arbutin and hydrophobic coumaric acid. *Food Chemistry, 300*, 125171.

Huang, G. Q., Sun, Y. T., Xiao, J. X., & Yang, J. (2012). Complex coacervation of soybean protein isolate and chitosan. *Food Chemistry, 135*(2), 534–539.

Jourdain, L. S., Schmitt, C., Leser, M. E., Murray, B. S., & Dickinson, E. (2009). Mixed layers of sodium caseinate+ dextran sulfate: Influence of order of addition to oil–water interface. *Langmuir, 25*(17), 10026–10037.

Kaushik, P., Dowling, K., Barrow, C. J., & Adhikari, B. (2015). Complex coacervation between flaxseed protein isolate and flaxseed gum. *Food Research International, 72*, 91–97.

Khalesi, H., Emadzadeh, B., Kadkhodaee, R., & Fang, Y. (2016). Whey protein isolate-Persian gum interaction at neutral pH. *Food Hydrocolloids, 59*, 45–49.

Lan, Y., Chen, B., & Rao, J. (2018). Pea protein isolate–high methoxyl pectin soluble complexes for improving pea protein functionality: Effect of pH, biopolymer ratio and concentrations. *Food Hydrocolloids, 80*, 245–253.

Liang, L. I., & Luo, Y. (2020). Casein and pectin: Structures, interactions, and applications. *Trends in Food Science & Technology, 97*, 391–403.

Li, J., Bhattacharjee, S., & Ghoshal, S. (2015). The effects of viscosity of carboxymethyl cellulose on aggregation and transport of nanoscale zerovalent iron. *Colloids and Surfaces A: Physicochemical and Engineering Aspects, 481*, 451–459.

Liu, G., & Zhong, Q. (2012). Glycation of whey protein to provide steric hindrance against thermal aggregation. *Journal of Agricultural and Food Chemistry, 60*(38), 9754–9762.

Li, N., & Zhong, Q. (2020a). Casein core-polysaccharide shell nanocomplexes stable at pH 4.5 enabled by chelating and complexation properties of dextran sulfate. *Food Hydrocolloids, 103*, Article 105723.

Li, N., & Zhong, Q. (2020b). *Stable casein micelle dispersions at pH 4.5 enabled by propylene glycol alginate following a pH-cycle treatment* (p. 115834). Carbohydrate Polymers.

Mekmene, O., & Gaucheron, F. (2011). Determination of calcium-binding constants of caseins, phosphoserine, citrate and pyrophosphate: A modelling approach using free calcium measurement. *Food Chemistry, 127*(2), 676–682.

Nunes, C. S., Rufato, K. B., Souza, P. R., de Almeida, E. A., da Silva, M. J., Scariot, D. B., et al. (2017). Chitosan/chondroitin sulfate hydrogels prepared in [Hmim][HSO_4] ionic liquid. *Carbohydrate Polymers, 170*, 99–106.

Orlien, V., Boserup, L., & Olsen, K. (2010). Casein micelle dissociation in skim milk during high-pressure treatment: Effects of pressure, pH, and temperature. *Journal of Dairy Science, 93*(1), 12–18.

Pan, K., & Zhong, Q. (2013). Improving clarity and stability of skim milk powder dispersions by dissociation of casein micelles at pH 11.0 and acidification with citric acid. *Journal of Agricultural and Food Chemistry, 61*(38), 9260–9268.

Patel, V. R., & Agrawal, Y. (2011). Nanosuspension: An approach to enhance solubility of drugs. *"Journal of Advanced Pharmaceutical Technology & Research"", 2*(2), 81.

Pitkowski, A., Nicolai, T., & Durand, D. (2008). Scattering and turbidity study of the dissociation of casein by calcium chelation. *Biomacromolecules, 9*(1), 369–375.

Rohart, A., Bouveresse, D. J.-R., Rutledge, D. N., & Michon, C. (2015). Spectrophotometric analysis of polysaccharide/milk protein interactions with methylene blue using independent components analysis. *Food Hydrocolloids, 43*, 769–776.

Saricay, Y., Hettiarachchi, C. A., Culler, M. D., & Harte, F. M. (2019). Critical phosphate salt concentrations leading to altered micellar casein structures and functional intermediates. *Journal of Dairy Science, 102*(8), 6820–6829.

Sejersen, M. T., Salomonsen, T., Ipsen, R., Clark, R., Rolin, C., & Engelsen, S. B. (2007). Zeta potential of pectin-stabilised casein aggregates in acidified milk drinks. *International Dairy Journal, 17*(4), 302–307.

Souza, C. J., & Garcia-Rojas, E. E. (2017). Interpolymeric complexing between egg white proteins and xanthan gum: Effect of salt and protein/polysaccharide ratio. *Food Hydrocolloids, 66*, 268–275.

Tafulo, P., Queirós, R. B., & González-Aguilar, G. (2009). On the "concentration-driven" methylene blue dimerization. *Spectrochimica Acta Part A: Molecular and Biomolecular Spectroscopy, 73*(2), 295–300.

Timilsena, Y. P., Wang, B., Adhikari, R., & Adhikari, B. (2016). Preparation and characterization of chia seed protein isolate–chia seed gum complex coacervates. *Food Hydrocolloids, 52*, 554–563.

Voron'ko, N. G., Derkach, S. R., Kuchina, Y. A., & Sokolan, N. I. (2016). The chitosan–gelatin (bio) polyelectrolyte complexes formation in an acidic medium. *Carbohydrate Polymers, 138*, 265–272.

Wagoner, T. B., & Foegeding, E. A. (2017). Whey protein–pectin soluble complexes for beverage applications. *Food Hydrocolloids, 63*, 130–138.

Walstra, P. (2002). *Physical chemistry of foods*. New York: CRC Press (Chapter 4)&6).

Wang, X., Nian, Y., Zhang, Z., Chen, Q., Zeng, X., & Hu, B. (2019a). High internal phase emulsions stabilized with amyloid fibrils and their polysaccharide complexes for encapsulation and protection of β-carotene. *Colloids and Surfaces B: Biointerfaces, 183*, Article 110459.

Wang, Y., Pillai, P. K., & Nickerson, M. T. (2019b). Effect of molecular mass and degree of substitution of carboxymethyl cellulose on the formation electrostatic complexes with lentil protein isolate. *Food Research International, 126*, Article 108652.

Xin, C., Nie, L., Chen, H., Li, J., & Li, B. (2018). Effect of degree of substitution of carboxymethyl cellulose sodium on the state of water, rheological and baking performance of frozen bread dough. *Food Hydrocolloids, 80*, 8–14.

Xiong, W., Ren, C., Li, J., & Li, B. (2018). Characterization and interfacial rheological properties of nanoparticles prepared by heat treatment of ovalbumin-carboxymethylcellulose complexes. *Food Hydrocolloids, 82*, 355–362.

Xiong, W., Ren, C., Tian, M., Yang, X., Li, J., & Li, B. (2017). Complex coacervation of ovalbumin-carboxymethylcellulose assessed by isothermal titration calorimeter and rheology: Effect of ionic strength and charge density of polysaccharide. *Food Hydrocolloids, 73*, 41–50.

Yang, Y., Anvari, M., Pan, C.-H., & Chung, D. (2012). Characterisation of interactions between fish gelatin and gum Arabic in aqueous solutions. *Food Chemistry, 135*(2), 555–561.